TECHNISCHE MECHANIK, 32, 2-5, (2012), 435 – 445
submitted: October 14, 2011

A Mechanism-Based Model for LCF/HCF and TMF/HCF Life Prediction: Multiaxial Formulation, Finite-Element Implementation and Application to Cast Iron

M. Metzger, T. Seifert

In this paper, the multiaxial formulation of a mechanism-based model for fatigue life prediction is presented which can be applied to low-cycle fatigue (LCF) and thermomechanical fatigue (TMF) problems in which high-cycle fatigue loadings are superimposed. The model assumes that crack growth is the lifetime limiting mechanism and that the crack advance in a loading cycle da/dN correlates with the cyclic crack-tip opening displacement $\Delta CTOD$. The multiaxial formulation makes use of fracture mechanics solutions and thus, does not need additional model parameters quantifying the effect of the multiaxiality. Furthermore, the model includes contributions of HCF on $\Delta CTOD$ and assesses the effect of the direction of the HCF loadings with respect to LCF or TMF loadings in the life prediction. The model is implemented into the finite-element program ABAQUS. It is applied to predict the fatigue life of a thermomechanically loaded notched specimen that should represent the situation between the inlet and outlet bore holes of cylinder heads. A good correlation of the predicted and the measured fatigue lives is obtained.

1 Introduction

Nowadays, cast iron materials are used in many high temperature components like cylinder heads and exhaust gas systems. These components are subjected to severe (thermo)mechanical loadings from start-up and shut-down, which lead to low cycle fatigue (LCF) and thermomechanical fatigue (TMF) of the material. Besides the (thermo)mechanical loadings, superimposed higher frequent loadings (high cycle fatigue, HCF) due to e.g. vibrations or ignition pressure are present. The superimposed HCF might contribute to additional damage and reduce the lifetime significantly. Thus, TMF as well as HCF must both be considered in the component design and the material choice to ensure the integrity of the component for a whole product life at the customer. There is a demand for reliable computational methods allowing the calculation of the lifetime of the components under LCF/HCF and TMF/HCF loading conditions, so that the components can be optimized via finite-element calculations. To this end, constitutive models for cast iron are required that are able to compute reliable stress and (plastic) strain fields. Moreover, lifetime models are needed, which make use of the stress and strain fields to estimate the cycles to failure.

Recently, a pressure dependent model including kinematic hardening was proposed in Seifert and Riedel (2010) and Seifert et al. (2010a) that is able to describe cyclic plasticity and tension/compression asymmetry of cast iron materials under TMF conditions. An efficient algorithm for this model was derived by the author of this work and was implemented in the finite-element software Hibbit et al. (2010), so that large-scale finite-element calculations can be carried out with the model to compute the stresses and plastic strains in components.

Reliable lifetime models for TMF problems are rare. Purely phenomenological lifetime models generally cannot reproduce the dependency of damage on the stress-temperature history appropriately. Furthermore, they do not consider the effect of superimposed HCF on the fatigue life. Recently, a mechanism-based model for LCF and TMF life prediction was proposed in Seifert and Riedel (2010) and Seifert et al. (2010b). The model assumes that under higher strain amplitudes in LCF and TMF cracks initiate in an early stage of the lifetime, so that the growth of cracks is the lifetime limiting factor. The basic assumption of the employed crack growth law is that the increment in crack advance per loading cycle da/dN is of the order of the cyclic crack-tip opening displacement $\Delta CTOD$. The model results in the damage parameter D_{TMF} proposed by Schmitt et al. (2002). The model can predict LCF and TMF fatigue lives of the cast iron materials EN GJS700, EN GJV450 and EN GJL250 very well, Seifert et al. (2010a). In Schweizer et al. (2011), crack growth in a 10 %-chromium steel for turbine shafts is

investigated unter LCF with superimposed HCF. They propose a LCF/HCF model for uniaxial loading situations which is also based on the correlation of da/dN and $\Delta CTOD$ and takes crack growth increments due to HCF loading cycles into account, as long as a threshold stress intensity factor is exceeded and the crack is open. In Metzger et al. (2011), the model of Schweizer et al. (2011) is extended to take the influence of an effective Young's modulus on the HCF stress range into account and combined with the model of Seifert and Riedel (2010). It results in a LCF/HCF and TMF/HCF model that can predict crack growth curves as well as fatigue lives measured in uniaxial tests with the cast iron materials EN GJS700, EN GJV450 and EN GJL250 very well. A multiaxial formulation and a finite-element implementation of the model is now necessary, so that the model can be applied to predict the fatigue life of components.

It was an aim of a German research project funded by the FVV (Research Association for Combustion Engines) to derive a multiaxial formulation of the mechanism-based model for LCF/HCF and TMF/HCF life prediction and to implement the model into a finite-element program. The model formulation and implementation should allow the evaluation of different HCF amplitudes and frequencies within the LCF or TMF cycle. The multiaxial model and the finite-element implementation are presented in this paper.

The paper is structured as follows: First, the multiaxial formulation of the mechanism-based fatigue life model for LCF and TMF is introduced, before the multiaxial formulation of the LCF/HCF and TMF/HCF model is derived. Then remarks on the finite-element implementation are given. The model is applied to predict the fatigue lives of uniaxial as well as experiments with low multiaxiality. Finally, the results are discussed and concluded.

2 A Mechanism-Based Model for LCF/HCF and TMF/HCF Life Prediction

2.1 Multiaxial Formulation of the Model for LCF and TMF

The mechanism-based model presented in Seifert and Riedel (2010) is based on the assumption that the cyclic crack tip opening displacement $\Delta CTOD$ correlates with the crack advance da per cycle dN

$$\frac{da}{dN} = \beta \Delta CTOD^B. \tag{1}$$

The exponent B is often in the order of one. The proportionality factor β can depend on microstructural quantities, as e.g. the volume fraction of the graphite inclusions in cast iron materials and quantities characterizing the graphite morphology. An analytical fracture mechanics based estimate of $\Delta CTOD$ for elastic-viscoplastic materials under arbitrary non-isothermal loading cycles is

$$\Delta CTOD = d_{n'} D_{TMF} a. \tag{2}$$

Therein, $d_{n'}$ depends on the hardening behavior of the material. For power-law hardening materials the crack-tip fields are the Hutchinson, Rice and Rosengren (HRR) singular fields (Hutchinson, 1968; Rice and Rosengren, 1968). In this case $d_{n'}$ is a function of the Ramberg-Osgood hardening exponent n' and was tabulated by Shih (1983) for plane strain and plane stress. D_{TMF} is the damage parameter of Schmitt et al. (2002) that is

$$D_{TMF} = \frac{Z_D}{\sigma_{CY}} F\left(t, \boldsymbol{\sigma}, \theta\right). \tag{3}$$

It comprises the damage parameter Z_D proposed by Heitmann et al. (1984) for room temperature applications and the function $F\left(t, \boldsymbol{\sigma}, \theta\right)$, that is a function of the stress-temperature-time history. σ_{CY} is the cyclic yield stress defined as the 0.2%-offset stress with respect to the point of load reversal. Z_D can be calculated from characteristic quantities of the stress-strain hysteresis loop. In this paper, the following multiaxial formulation of Z_D for a semicircular surface crack loaded in mode I is employed

$$Z_D = 1.45 \frac{\left(\Delta\sigma_{I,eff}\right)^2}{E} + \frac{2.4}{\sqrt{1+3n'}} \frac{\Delta\sigma_I^2 \Delta\varepsilon_e^{in}}{\Delta\sigma_e}. \tag{4}$$

E is Young's modulus. ε^{in} is the inelastic strain. The form of Z_D goes back to the work of Kumar et al. (1981), who approximated the J integral by a sum of an elastic and a plastic part, and of He and Hutchinson (1981), who developed an approximate solution for the J integral of a penny shaped crack in power-law materials within the plastic limit. The indices I and e denote the principal and the von Mises equivalent value of the respective quantity.

If in multiaxial loading situations the direction of the maximal principal stress strongly changes within the LCF or TMF loading cycle, mixed mode hypothesis might be required such as e.g. proposed by Hoffmeyer et al. (2006). However, if the degree of non-proportionality is small, the direction of the maximal principal stress does not change significantly between the points of load reversal. In this case, the following definitions for the stress and strain ranges can be employed

$$\Delta\sigma_I = \left|\sigma_H^1 - \sigma_H^0\right| \text{ where } \sigma_H^1 = \boldsymbol{n}^0 \cdot \boldsymbol{\sigma}^1 \cdot \boldsymbol{n}^0 \tag{5}$$

$$\Delta\sigma_e = (\boldsymbol{\sigma}^1 - \boldsymbol{\sigma}^0)_e \tag{6}$$

$$\Delta\epsilon_e^{in} = (\boldsymbol{\epsilon}^{in,1} - \boldsymbol{\epsilon}^{in,0})_e. \tag{7}$$

The subscript 0 and 1 indicate the points of load reversal, 0 is the starting point. σ_H is the largest principal stress referred to its absolute value, i.e. $\sigma_H = \max(|\sigma_I|, |\sigma_{III}|)$. $\boldsymbol{n}_0$ is the principal direction corresponding to σ_H^0, which is the normal on the crack faces.

Crack closure is accounted for in the elastic part of Z_D, where the stress range is replaced by an effective stress range. In this work, the crack closure model of Newman (1984) is used and formulated for multiaxial stress states. The model predicts decreasing crack opening stresses σ_{OP} at larger maximum stresses

$$\sigma_{max} = \max\left(\sigma_H^1, \sigma_H^0\right), \tag{8}$$

so that the effective stress range

$$\Delta\sigma_{I,eff} = \sigma_{max} - \sigma_{OP} \tag{9}$$

increases. Besides the maximum stress, the stress ratio R_σ enters the model, which is computed from

$$R_\sigma = \begin{cases} \sigma_H^0/\sigma_H^1 & \text{if } \sigma_H^1 > \sigma_H^0 \\ \sigma_H^1/\sigma_H^0 & \text{else} \end{cases}. \tag{10}$$

The case differentiation is introduced to distinguish whether the loading or unloading curve of the hysteresis loop is considered. The equations of the Newman model are

$$\frac{\sigma_{OP}}{\sigma_{max}} = A_0 + A_1 R_\sigma + A_2 R_\sigma^2 + A_3 R_\sigma^3 \text{ if } R_\sigma \geq 0 \tag{11}$$

$$\frac{\sigma_{OP}}{\sigma_{max}} = A_0 + A_1 R_\sigma \text{ if } -1 \leq R_\sigma < 0 \tag{12}$$

$$A_0 = 0.535\left(\cos(\frac{\pi\sigma_{max}}{\sigma_{CY}})\right) \tag{13}$$

$$A_1 = 0.688\frac{\sigma_{max}}{\sigma_{CY}} \tag{14}$$

$$A_3 = 2A_0 + A_1 - 1 \tag{15}$$

$$A_2 = 1 - A_0 - A_1 - A_3. \tag{16}$$

The function $F(t, \boldsymbol{\sigma}, \theta)$ in equation (3) contains the activation energy for creep Q, Norton's stress exponent m and a stress dependent function h, which includes an adjustable parameter α

$$F = \left(1 + \int_t h(\boldsymbol{\sigma}) \exp -\frac{Q}{\bar{R}\theta} dt\right)^{1/m}. \tag{17}$$

$\bar{R}$ is the gas constant and θ the temperature in Kelvin. For time independent material behavior $F = 1$ holds.

For non-isothermal cycles, Schmitt et al. (2002) found good fatigue life predictions if D_{TMF} is taken as the average of the values calculated for the rising and the falling temperature branch. This choice is reasonable since the points of reversal of temperature and $\Delta CTOD$ coincide (Schweizer et al., 2007). To take the temperature dependency of the material parameters into account, the arithmetic mean of the minimal and the maximal value occurring in a branch is used for the evaluation of D_{TMF}.

2.2 Multiaxial Formulation of the Model for LCF/HCF and TMF/HCF

To account for the effect of superimposed HCF loads within a LCF or TMF cycle on the fatigue life, the model presented in the previous section is extended according to the uniaxial LCF/HCF and TMF/HCF model proposed in Metzger et al. (2011) and formulated in the context of multiaxial loading conditions. To this end, the total crack advance per cycle is expressed as the sum of the total (peak-to-peak) loading cycle and the sum of all HCF cycles during one LCF or TMF cycle, respectively

$$\frac{da}{dN} = \left.\frac{da}{dN}\right|^{LCF,TMF} + \sum \left.\frac{da}{dN}\right|^{HCF} . \tag{18}$$

The first term on the right side is given by

$$\left.\frac{da}{dN}\right|^{LCF,TMF} = \beta \left(\Delta CTOD|^{LCF,TMF}\right)^B = \beta \left(d_{n'} D_{TMF} a\right)^B . \tag{19}$$

In engineering applications the HCF loadings are usually small. Thus, it is assumed that only elastic unloadings take place within the HCF cycle so that the superimposed crack advance is estimated using the elastic part of Z_D

$$\left.\frac{da}{dN}\right|^{HCF} = \beta \left(\Delta CTOD|^{HCF}\right)^B = \beta \left(d'_n 1.45 \frac{(\Delta\sigma^{HCF}_{I,eff})^2}{E\sigma_{CY}} a \right)^B G. \tag{20}$$

However, the HCF loads only contribute to the opening of the crack, if the stress range tensor due to the HCF loads $\Delta\boldsymbol{\sigma}^{HCF}$ has a component in direction of the normal to the crack faces, hence

$$\Delta\sigma^{HCF}_I = \boldsymbol{n}^0 \cdot \Delta\boldsymbol{\sigma}^{HCF} \cdot \boldsymbol{n}^0. \tag{21}$$

Moreover, the opening of the crack is only affected by superimposed HCF if the crack is actually open. Thus, it is assumed that the maximal stress in the HCF cycle σ^{HCF}_{max} must be greater than the crack opening stress σ_{OP} of the LCF or TMF cycle, so that equation (20) is taken nonzero only if

$$\sigma^{HCF}_{max} \geq \sigma_{OP}. \tag{22}$$

Finally, the experimental results of Schweizer et al. (2011) and Metzger et al. (2011) indicate that crack growth is only accelerated by superimposed HCF loadings if the effective stress intensity factor range in a HCF cycle (small semicircular surface crack)

$$\Delta K^{HCF}_{I,eff} = \frac{2.243}{\pi} \Delta\sigma^{HCF}_{I,eff} \sqrt{\pi a} \tag{23}$$

exceeds an effective threshold of the stress intensity factor range $\Delta K^{HCF}_{I,th,eff}$. Equation (20) is therefore only nonzero if

$$\Delta K^{HCF}_{I,eff} \geq \Delta K^{HCF}_{I,th,eff}. \tag{24}$$

The function G in equation (20) accounts for the behavior in the near threshold regime and is taken as (Newman, 1981)

$$G = 1 - \left(\frac{\Delta K^{HCF}_{I,th,eff}}{\Delta K^{HCF}_{I,eff}} \right)^p . \tag{25}$$

The parameter p must be determined on the basis of crack growth curves.

Integration of equation (18) from an initial crack length a_0 to a crack length a_f, where failure is defined, yields the number of cycles to failure. The integration requires a critical crack length a_{cr}, at which the effective threshold is exceeded and HCF contributes to crack growth

$$a_{cr} = \left(\Delta K^{HCF}_{I,th,eff} \frac{\sqrt{\pi}}{2.243 \Delta\sigma^{HCF}_{I,eff}} \right)^2 . \tag{26}$$

For a linear relation between the crack advance per cycle and the crack tip opening displacement ($B = 1$), equation (18) yields

$$\frac{da}{dN} = k_4 a - k_3 a^{1-\frac{p}{2}} \tag{27}$$

$$k_4 = \beta d_{n'} D_{TMF} + \beta d_{n'} \sum 1.45 \frac{(\Delta\sigma_{I,eff}^{HCF})^2}{E\sigma_{CY}} = k_1 + k_2 \tag{28}$$

$$k_3 = k_2 \left(\frac{\Delta \bar{K}_{I,th,eff}}{\frac{2.243}{\sqrt{\pi}} (\Delta\bar{\sigma}_{I,eff}^{HCF})^2}\right). \tag{29}$$

Due to the dependence of Young's modulus on the temperature and the evolution of microstructural quantities as e.g. the volume of the graphite precipitations in cast iron, $K_{I,th,eff}$ and $\Delta\sigma_{I,eff}^{HCF}$ might change within one LCF or TMF cycle. Hence, their mean value $\bar{(\cdot)}$ is computed and used in the integration of the crack growth law.

For the case $a_{cr} < a_0$ the cycles to failure are

$$N_f = \frac{p\ln(a_f) + 2\ln(k_3 a_f^{\frac{-p}{2}} - k_4) - p\ln(a_0) - 2\ln(k_3 a_0^{\frac{-p}{2}} - k_4)}{k_4 p}. \tag{30}$$

If $a_0 \leq a_{cr} < a_f$ holds, then the cycles to failure are computed additively by

$$N_f = \frac{\ln(\frac{a_{cr}}{a_0})}{k_1} + \frac{p\ln(a_f) + 2\ln(k_3 a_f^{\frac{-p}{2}} - k_4) - p\ln(a_{cr}) - 2\ln(k_3 a_{cr}^{\frac{-p}{2}} - k_4)}{k_4 p}. \tag{31}$$

If $a_f \leq a_{cr}$ holds, then HCF does not reduce the lifetime and the cycles to failure are

$$N_f = \frac{\ln(\frac{a_f}{a_0})}{k_1}. \tag{32}$$

For $B > 1$, the crack growth law is integrated numerically.

2.3 Finite-Element Implementation of the Mechanism-Based Model for LCF/HCF and TMF/HCF Life Prediction

The described mechanism-based model for LCF/HCF and TMF/HCF life prediction was implemented into the finite-element program ABAQUS and extends the implementation of the constitutive deformation model. For the lifetime evaluation, saturated LCF or TMF hysteresis are required. Typically three LCF or TMF loading cycles are computed and the third cycle is used for the fatigue life evaluation. The points of load reversal are defined in the third cycle, so that the strain and stress ranges of equations (5) to (7) can be calculated.

To determine the HCF stress range $\Delta\boldsymbol{\sigma}^{HCF}$ in equation (21), one or several HCF cycles are computed in the third LCF or TMF loading cycle. The stress range and frequency of a computed HCF cycle is kept constant for the following HCF cycles until a new HCF cycle is again computed. If several HCF cycles are considered, varying frequencies and amplitudes can be taken into account. In components however, HCF can enlarge the range of the stresses and strains between the points of load reversal of the LCF or TMF hysteresis. To take an enlarged hysteresis into account in the computation of $\Delta CTOD|^{LCF,TMF}$ (equation 19), $\Delta\sigma_I^{HCF}$ is computed at least twice per loading branch (at the beginning and the end) to ensure the correct computation of the maximal stress and strain range. The sum over all HCF cycles in equation (18) is replaced by a sum over all time increments Δt_i required in the calculation of the LCF or TMF loading cycle

$$\sum \rightarrow \sum_i f_i \Delta t_i. \tag{33}$$

f_i is the current frequency of the HCF load in the time increment Δt_i.

Under strain controlled loading, the HCF stress range might change within a LCF or TMF loading cycle, since Young's modulus depends on temperature and, for cast iron materials, on other microstructural quantities. Under strain controlled loading the HCF stress range $\Delta\sigma_I^{HCF}$ is therefore computed from the HCF stress range $\Delta\sigma_I^{HCF^*}$, which was computed at a certain temperature (Young's modulus E^*), and from the Young's modulus E corresponding to the current temperature

$$\Delta\sigma_I^{HCF} = \frac{E}{E^*} \Delta\sigma_I^{HCF^*}. \tag{34}$$

In equation (22) σ_{max}^{HCF} is computed within each time increment $\Delta t = t_{n+1} - t_n$ that is

$$\sigma_{max}^{HCF} = \sigma_{H^*}^{t_n} + (\sigma_{H^*}^{t_{n+1}} - \sigma_{H^*}^{t_n}) \frac{j}{\Delta t \cdot f}, \tag{35}$$

where j the control variable running from 1 to $\Delta t \cdot f$. The index * accounts for the case that superimposed HCF might enlarge σ_H. Then,

$$\sigma_{H^*} = \sigma_H + \Delta\sigma_I^{HCF} \tag{36}$$

is used. Else, for the case of HCF unloading $\sigma_{H^*} = \sigma_H$ is used.

3 Comparison of Model Predictions with Experimental Results

In this section, the proposed model is applied to predict the fatigue lives of experiments. As it was the case in the formulation of the model, it is assumed here that in the HCF loading cycles only elastic unloading occurs. For the considered HCF conditions this is a reasonable assumption, since the stresses and strains are not altered due to superimposed HCF loadings (Metzger et al., 2011). Thus, the constitutive model of Seifert and Riedel (2010) for pure TMF and the TMF/HCF fatigue life model can be applied.

3.1 Uniaxial Experiments

In cooperation with the Karlsruhe Institute of Technology KIT several uniaxial LCF and TMF tests with and without superimposed HCF and dwell times have been performed with the cast iron EN GJS700 (Uihilein et al., 2008; Heritier et al., 2011). The parameters of the deformation model adjusted in Uihilein et al. (2008) are also used in this work so that Z_D can be calculated from a saturated stress strain hysteresis. The parameters of the function F are: Q/R=1.68e+4 K, α=1.51e-10 1/MPa^{2}s, m=4.

On the basis of the experimental results, the model parameters of the presented LCF/HCF and TMF/HCF model were determined. The initial crack depth a_0 was chosen to be 20μm that correlates approximately with the diameter of the graphite inclusions and the first cracks that were experimentally measured on the surface in LCF tests (Metzger et al., 2011; Heritier et al., 2011). The crack growth law is then integrated until 1000μm, where the crack depth at failure a_f is defined. The proportionality constant between crack opening and growth β is 0.394 and the exponent B is 1.5. Typically, for equal values B, the shape of the microstructure in cast iron should be represented in β (Metzger et al., 2011) in the sense that β increases with an increasing internal stress intensity factor or characteristic length (e.g. compare spherical and lamellar graphite precipitations). The exponent p of the transition function is 0.5 and the effective threshold is taken to be $\Delta K_{I,th,eff}^{HCF}$ = 5.9e-6 $\cdot E$. Therein, E depends on the actually computed value of Young's modulus regarding the temperature and the microstructural evolution (Metzger et al., 2011). The maximal value E=172843MPa is given at room temperature (Uihilein et al., 2008) that yields a lower threshold than typically observed in test with CT specimens.

In Figure 1 and 2, the predicted $N_{f,sim}$ and experimentally measured lifetimes $N_{f,exp}$ are plot in a log-log scale that is normalized by the largest experimental number of cycles to failure. For the lifetime prediction the computed stress-strain hysteresis are used. Closed symbols describe experiments that have been performed at Fraunhofer Institute for Mechanics of Materials IWM in Freiburg. Open symbols correspond to fatigue tests performed at the KIT. The dashed lines define a scatter-band of factor two.

A constant strain rate of 0.001 1/s was used in the LCF tests of Fraunhofer IWM. The TMF tests were performed at fully constraint total strains. A temperature rate of 10 K/s was used for heating up and cooling down. The frequency of the superimposed HCF cycles was 50 Hz. In tests at Fraunhofer IWM, the maximal and minimal mechanical strains for one temperature (LCF) or temperature range (TMF) were equal to those of the corresponding LCF/HCF or TMF/HCF tests. The enveloping stress-strain hysteresis loops of LCF and LCF/HCF tests as well as of TMF and TMF/HCF tests were almost the same, indicating that the HCF cycles are elastic as assumed in the model (Metzger et al., 2011).

The LCF tests at KIT were performed with a frequency of 1 Hz independently of the strain amplitude and a superimposed HCF load with a frequency of 5 Hz was used. The temperature rate applied in the TMF tests was 10 K/s at fully constraint total strains. In the LCF/HCF and TMF/HCF tests, the superimposed HCF amplitude was added to the basic LCF or TMF total strains. Hence, the range of the mechanical strains of the LCF or TMF hysteresis increase by the HCF strain amplitude. The symbols with an additional cross describe TMF(/HCF) tests

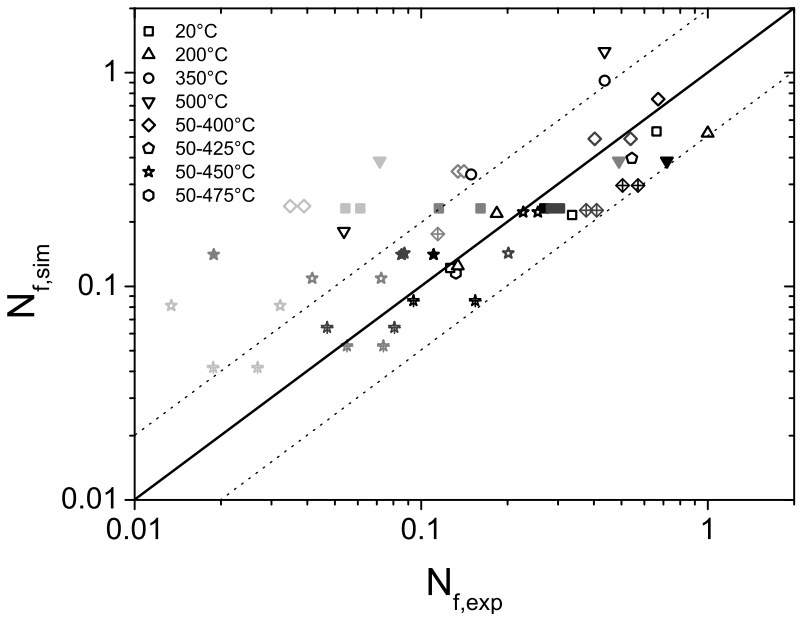

Figure 1: Lifetime prediction EN GJS700: HCF is neglected

with 60 seconds dwell time at minimal total strains. Black symbols denote experiments without superimposed HCF. Dark gray, gray and light gray symbols represent an increasing superimposed HCF range.

Figure 1 shows the lifetime prediction for the case that the influence of superimposed HCF on the fatigue life is not taken into account. Thus the model predicts higher fatigue lives than observed in the experiments. Considering the additive damage due to superimposed HCF, the model is able to predict the cycles to failure for all experiments quite well (see Figure 2).

3.2 Experiments with Notched Specimen

A notched specimen, which resembles the geometric situation between the inlet and outlet bore holes in cylinder heads, was tested under TMF and TMF/HCF loading. In the gauge length the thermal strains due to thermal cycling were fully suppressed. In the TMF/HCF tests, HCF was induced strain controlled. A temperature gradient was applied in the specimen as described in Heritier et al. (2011). The geometrical dimensions of the specimen were defined such that the notch radius is equal to the width of the ligament. The notch radius is 4 mm.

In the tests, the maximal load in tension and the stiffness of the specimen were recorded as indication for growing fatigue cracks. Two significant points were observed in the stiffness evolution. After coalescence of the several microcracks, that mainly started from the spherically shaped graphite precipitations, a first discontinuity (S_1) was measured and a crack of few hundred microns was detected as shown in the micrograph in Figure 3(a). A second discontinuity (S_2) was observed after the specimen failed almost completely. The number of cycles at the respective points are used to validate the proposed multiaxial TMF/HCF model. The predicted number of cycles to failure should lie between S_1 and S_2. Figure 3(b) shows the fracture surface. The dark area is the oxidized crack face (marked with a dashed line). The crack started at the hot side of the specimen.

First, the temperature fields in the specimen are computed in a finite-element calculation. Due to symmetry, only one quarter of the specimen needs to be modeled between the strain gauge. For the calculation of the temperature fields, results of temperature measurements were used as boundary conditions: in the experiment, two measure points were applied on the hot and two at the cool side of the specimen. At each measured instant of time, the temperature field between the measure points was obtained by linear interpolation, so that a transient temperature field is obtained. Since the specimen was heated by induction, the temperatures at the hot side of the specimen were kept constant up to a depth of 1 mm to approximately reproduce the skin effect in inductively heated specimens. Figure 4(a) shows the peak temperature distribution. In the second step, the transient temperature fields were applied to compute the stresses and (plastic) strains in the specimen using the constitutive model. These results

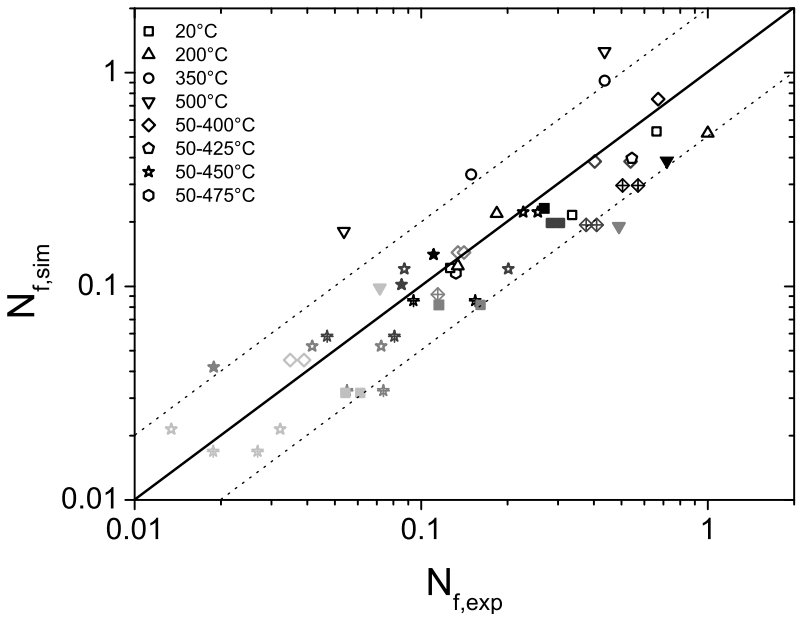

Figure 2: Lifetime prediction EN GJS700: HCF is considered

are then used in the last step to evaluate the fatigue life with the multiaxial model for TMF/HCF life prediction proposed in this paper.

The finite-element model predicts the critical location in the specimen, where also in the experiment the cracks are observed, see Figure 4(b). In Figure 5, the experimentally measured cycles until S_1(rectangles) and S_2(triangles) and numerically computed cycles to failure (surface crack with 1mm depth) are plot; normalized by the maximal experimentally measured cycles to failure. Open, black symbols denote TMF tests without superimposed HCF, whereas the closed black, dark gray, gray and light gray data describe TMF/HCF with an increasing amplitude. A large scatter is observed in the TMF tests. Specimens tested without superimposed HCF partly even show lower fatigue lifes than specimen tested with superimposed HCF which is assumed to be due to scatter and cannot explained with the model. The model predicts the fatigue lives of TMF/HCF and the TMF tests with larger values of S_1 and S_2 well, where most of the predicted fatigue lives fall into the scatter-band with factor of two. The reason for the large scatter in the TMF experiments and their partly low values of S_1 was not clarified.

From the integration point with the lowest computed cycles to failure, the maximal principal stress at the cold stage drops by about 20% within the first millimeter in crack depth (along x-axis) for the TMF test. The factor for multiaxility (T_f) defined by the hydrostatic stress divided by the von Mises equivalent stress is equal to $-1/3$ under uniaxial tensile loading. At the integration point that predicts the lowest amount of cycles to failure, the stress state is almost uniaxial with $T_f = -0.36$ and $\sigma_H = 288MPa$. The largest absolute value of T_f in the x-y symmetry plane is approximately $|-0.7|$ with $\sigma_H = 250MPa$.

4 Discussion

In this paper a multiaxial formulation of the mechanism-based LCF/HCF and TMF/HCF model is derived which is based on fracture mechanics results. To this end, the cyclic crack-tip opening displacement $\Delta CTOD$, which drives crack growth in the model, is estimated using an approximation of the cyclic J-integral for semi-circular surface cracks under multiaxial loadings. Thus, the effect of multiaxial stress states can be included as a result of a mechanism-based view on crack growth. There are no additional model parameters necessary that must be adjusted to experimental data from multiaxial tests. All model parameters can be determined from uniaxial fatigue tests. Because the multiaxial stress state was quite low at the critical area of the notched specimen the model predictive capability at high multiaxiality remains uncertain. On the other hand, this means that the stress state at the critical area of the notched specimen differs only slightly from the uniaxial stress state of the experiments shown in Figure 2. Furthermore, the stress gradient at the critical area is still relatively small. Thus, the cycles to failure predicted

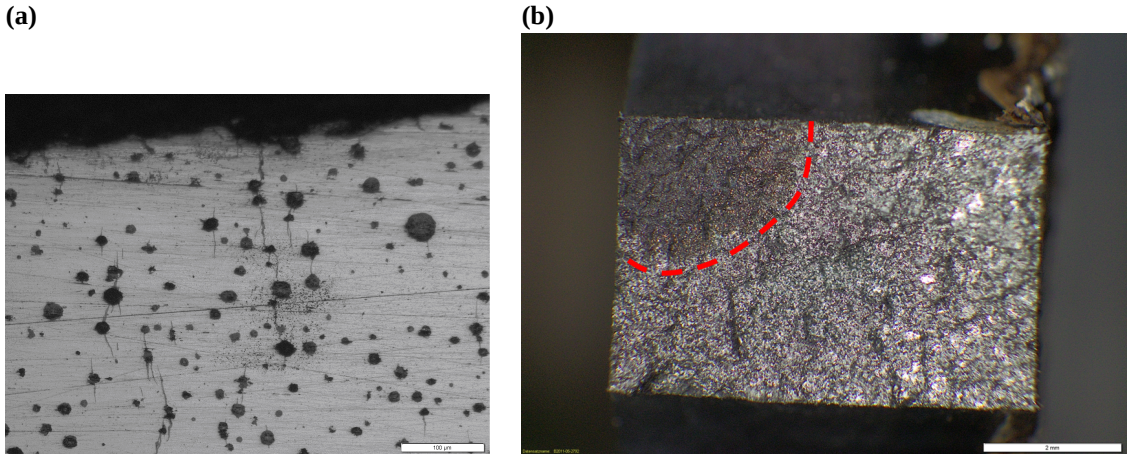

Figure 3: (a) Surface crack after first stiffness decay, (b) fracture surface with crack (black area), (Heritier et al., 2011)

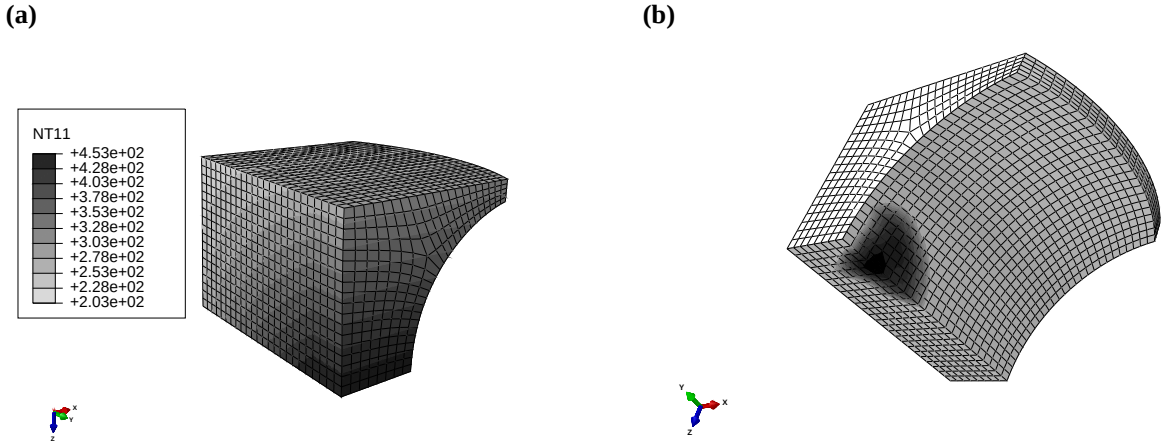

Figure 4: (a) Temperature distribution at hot stage: constant temperature within first millimeter, (b) critical area (dark) predicted in the finite-element calculation

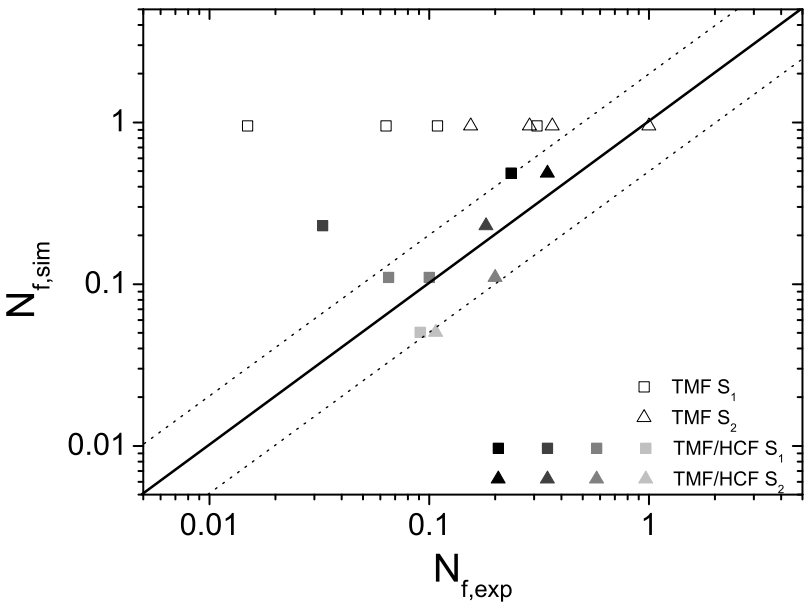

Figure 5: Lifetime prediction EN GJS700: TMF and TMF/HCF

between the inlet and outlet bore holes of cylinder heads under TMF or TMF/HCF should offer a similar quality as the predictions under uniaxial stress states.

For the lifetime evaluation in components, one crucial point is the computation and/or the measurement of a realistic temperature distribution. Furthermore, different cooling rates are often present within the casting process of components. Hence, varying microstructural morphologies of the graphite precipitations might evolute so that differences in physical and mechanical properties can be present and influence the lifetime behavior. This is still an open issue and could be addressed in future research projects.

Furthermore, no fracture mechanics theory exists to evaluate the cyclic J-integral for non-proportional loadings. In this paper, it is assumed that the degree of non-proportionality is low, which was found to be a reasonable assumption for thermomechanically loaded exhaust manifolds (Seifert, 2008) and seems also to be valid for the region between inlet and outlet valve in a cylinder head. In principle, also mixed mode approaches as well as phenomenological approaches for non-proportional loadings, as, e.g., the critical plane approach for finding maximum of the damage parameter in a loading cycle, can be used in combination with this model. However, it is desirable to find mechanism-based approximations by e.g. finite-element calculations of non-proportionally loaded cracks.

The model assumes that LCF or TMF loading, where relatively large strain amplitudes arise, leads to early crack initiation. The orientation of the crack is thus determined by the LCF or TMF load, i.e. by the crack normal $\boldsymbol{n^0}$ corresponding to the principal direction of the maximum principal stress. According to the model, a HCF load, which solely "acts perpendicular to the LCF load", will thus not reduce to fatigue life under LCF/HCF or LCF/TMF. This assumption seems to be plausible. However, in the notched specimen test used for the validation of the model in this paper, HCF and TMF act almost in the same direction. Hence, the influence of different directions could not be investigated and the experimental validation of this assumption of the model is still an open issue.

5 Conclusion

The presented mechanism-based LCF/HCF and TMF/HCF model can be applied to predict the fatigue lives of components under non-isothermal loading conditions. The model parameters can be determined on the basis of uniaxial fatigue tests and used in finite-element simulations to optimize high temperature components and, thus, to reduce the number of expensive and time-consuming bench and field tests.

References

He, M. Y.; Hutchinson, J. W.: The penny-shaped crack and the plane strain crack in an infinite body of power-law material. *J. Appl. Mech.*, 48, (1981), 830 – 840.

Heitmann, H. H.; Vehoff, H.; Neumann, P.: Life prediction for random load fatigue based on the growth behavior of microcracks. *Advances in Fracture Research 84 - Proc. of ICF6. Oxford/ New York: Pergamon Press Ltd.*, 5, (1984), 599 – 606.

Heritier, L.; Lang, K.-H.; Metzger, M.; Nieweg, B.; Brontfeyn, Y.; Tandler, M.; Schweizer, C.: *TMF/HCF - Lebensdauervorhersage Eisenguss*. Abschlussbericht FVV Vorhaben Nr. 985, Heft 947, Frankfurt am Main (2011).

Hibbit, D.; Karlson, B.; Sorensen, P.: *ABAQUS/Standard Manual, Version 6.10*. Dassault Systèmes Corp., Providence, RI, USA (2010).

Hoffmeyer, J.; Döring, R.; Seeger, T.; Vormwald, M.: Deformation behaviour, shortcrack growth and fatigue lives under multiaxial nonproportional loading. *Int. J. Fat.*, 28, (2006), 508 – 520.

Hutchinson, J. W.: Singular behaviour at the end of a tensile crack in a hardening material. *J. Mech. Phys. Sol.*, 16, (1968), 13 – 31.

Kumar, V.; German, M. D.; Shih, C. F.: *An engineering approach for elastic-plastic fracture analysis*. Tech. rep. NP-1931 on Project 1237-1, Electric Power Research Institute, Palo Alto California (1981).

Metzger, M.; Nieweg, B.; Schweizer, C.; Seifert, T.: Lifetime prediction of cast iron materials under combined thermomechanical fatigue and high cycle fatigue loading using a mechanism-based model. *Int. J. Fat.*, under review.

Newman, J. C.: A crack-closure model for predicting fatigue crack growth under aircraft spectrum loading. *In: Chang, J.B.; Hudson, C.M., editors. Methods and models for predicting fatigue crack growth under random loading, ASTM STP. American Society for Testing of Materials*, 748, (1981), 53 – 84.

Newman, J. C.: A crack opening stress equation for fatigue crack growth. *Int. J. Fract.*, 24, (1984), 131 – 135.

Rice, J. R.; Rosengren, G. F.: Plane strain deformation near a crack tip in a power law hardening material. *J. Mech. Phys. Sol.*, 16, (1968), 1 – 12.

Schmitt, W.; Mohrmann, R.; Riedel, H.; Dietsche, A.; Fischersworring-Bunk, A.: Modelling the fatigue life of automobile components. *Fatigue 2002 - Proceedings of the Eighth International Fatigue Congress held 3-7 june 2002, Stockholm, Sweden (Ed. A.F. Blom)*.

Schweizer, C.; Seifert, T.; Nieweg, B.; von Hartrott, P.; Riedel, H.: Mechanisms and modelling of fatigue crack growth under combined low and high cycle fatigue loading. *Int. J. Fat.*, 33, (2011), 194 – 202.

Schweizer, C.; Seifert, T.; Schlesinger, M.; Riedel, H.: Korrelation zwischen zyklischer Rissspitzenöffnung und Lebensdauer. *DVM-Bericht*, 239, (2007), 237ff.

Seifert, T.: *Computational methods for fatigue life prediction of high temperature components in combustion engines and exhaust systems - Dissertation*. Shaker Verlag GmbH, D-52018 Aachen (2008).

Seifert, T.; Maier, G.; Uihlein, A.; Lang, K.-H.; Riedel, H.: Mechanism-based thermomechanical fatigue life prediction of cast iron. Part II: Comparison of model prediction with experiments. *Int. J. Fat.*, 32, (2010a), 1368 – 1377.

Seifert, T.; Riedel, H.: Mechanism-based thermomechanical fatigue life prediction of cast iron. Part I: Models. *Int. J. Fat.*, 32, (2010), 1358 – 1367.

Seifert, T.; Schweizer, C.; Schlesinger, M.; Möser, M.; Eibl, M.: Thermomechanical fatigue of 1.4849 cast steel - experiments and life predicition using a fracture mechanics approach. *Int. J. Mat. Res.*, 101, (2010b), 942 – 950.

Shih, C. F.: Tables of Hutchinson-Rice-Rosengren singular field quantities. *J. Mech. Phys. Sol.*, Tech. rep. Brown University Report MRL E-147, (1983), 1 – 5.

Uihilein, A.; Lang, K.-H.; Seifert, T.; Riedel, H.; Mohrmann, R.; Maier, G.: *TMF - Lebensdauerberechnung Eisenguss*. Abschlussbericht FVV Vorhaben Nr. 825, Heft 860, Frankfurt am Main (2008).

Address:
Mario Metzger, M.Sc., Fraunhofer Institute for Mechanics of Materials IWM Freiburg, D-79108 Freiburg.
email: `mario.metzger@iwm.fraunhofer.de.`
Prof. Dr.-Ing. Thomas Seifert, University of Applied Sciences Offenburg, D-77652 Offenburg.
email: `thomas.seifert@hs-offenburg.de.`